Nonlinear interaction of compressional waves in a 2D dusty plasma crystal

V. Nosenko*, K. Avinash, J. Goree, and B. Liu

Department of Physics and Astronomy, The University of Iowa, Iowa City Iowa 52242

(May 30, 2003)

Abstract

Nonlinear mixing and harmonic generation of compressional waves were studied in a 2D Yukawa (screened Coulomb) triangular lattice. The lattice was a monolayer of highly charged polymer microspheres levitated in a plasma sheath. Two sinusoidal waves with different frequencies were excited in the lattice by pushing the particles with modulated Ar^+ laser beams. Waves at the sum and difference frequencies and harmonics were observed propagating in the lattice. Phonons interacted nonlinearly only above an excitation-power threshold due to frictional damping, as predicted by theory.

PACS number(s): 52.27.Lw, 82.70.Dd, 52.35.Mw, 52.27.Gr

*Electronic mail: vladimir-nosenko@uiowa.edu

Two-dimensional ordered lattices are found in variety of physical systems, including Langmuir monolayers [1], electrons on the surface of liquid helium [2], rare gas atoms absorbed on graphite [3], colloidal suspensions [4], and dusty plasmas [5–8]. In the latter two examples, particles interact through a screened Coulomb repulsion or Yukawa potential.

Sound waves, or phonons, in a 2D Yukawa lattice are well-studied in the linear or low-amplitude limit, both theoretically and experimentally. There are two kinds of waves, compressional and transverse, and at high frequency they exhibit dispersion, i.e., the frequency ω is not proportional to wavenumber k. However, for low frequencies $\omega < 1.3\omega_0$, the propagation of linear compressional sound waves is dispersionless [4,9,10], with a speed $C_L = \omega/k$ given in Ref. [9]. Here, $\omega_0^2 = Q^2/4\pi\epsilon_0 m a^3$ is a 2D analog of plasma frequency, where Q and m are the particle charge and mass, respectively, and a is the interparticle spacing.

A dusty plasma is a convenient model system to study waves in 2D lattices. Micron-size particles become highly charged when suspended in a plasma. Due to mutual repulsion and the plasma's weaker radial electric fields, they arrange themselves in a regular pattern with crystalline or liquid-like order. In the presence of gravity the particles can settle in a 2D monolayer. The particles can be imaged directly, and their positions and velocities calculated, which allows studying the lattice microscopically.

The properties of nonlinear waves have not been studied as completely as for linear waves, in dusty plasmas. It has been shown theoretically that nonlinear pulses can take the form of solitons [11–13] although frictional gas damping can suppress soliton formation [13]. In experiments with large amplitudes, nonlinear pulses [12,14] and harmonic generation [15] have been observed in 2D lattices.

Here, we report an experimental observation of nonlinear three-wave mixing in a 2D dusty plasma crystal, and a corresponding theory for a 2D Yukawa lattice. The experimental conditions for our particles were similar to those in Ref. [16], where the interparticle potential was experimentally shown to be nearly Yukawa, $U(r) = Q(4\pi\epsilon_0 r)^{-1}\exp(-r/\lambda_D)$, where λ_D is the Debye length. A lattice is characterized by the screening parameter $\kappa = a/\lambda_D$. Our plasma crystal had a triangular structure with hexagonal symmetry.

The three-wave mixing problem we investigate in a 2D triangular lattice has two externally-excited compressional pump waves. They have frequencies $\omega_1 < \omega_2$, and wavevectors $\mathbf{k}_1$ and $\mathbf{k}_2$, respectively. The waves propagate along a common axis and have parallel wave fronts. We analyze three-wave nonlinear mixing, resulting in the generation of the waves with combination frequencies $\omega_{\rm sum} = \omega_1 + \omega_2$ and $\omega_{\rm diff} = \omega_2 - \omega_1$, and second harmonic generation $\omega_{\rm sum} = 2\omega_1$ or $2\omega_2$.

In general, three-wave mixing requires satisfying the phase-matching conditions $\mathbf{k}_{\rm sum} = \mathbf{k}_1 + \mathbf{k}_2$ and $\mathbf{k}_{\rm diff} = \mathbf{k}_2 - \mathbf{k}_1$. Moreover, all the waves involved should satisfy the dispersion relation. For waves propagating along a common axis in a 2D Yukawa lattice, these conditions require that all the waves travel in the same direction and have wavelengths long enough to satisfy the wave's dispersion relation in its acoustic limit, where $\omega \propto k$. However, as we discuss later, these matching conditions are relaxed under some experimental conditions.

Our theory is based on the 1D chain model developed in Ref. [13]. This theory is applicable to waves propagating along a common axis in a 2D lattice.

Our model begins with a nonlinear equation of motion taking damping into account, Eq. 15 of Ref. [13]. This includes a binary interaction with four nearest neighbors and retains the linear and quadratic nonlinear terms after expanding the interparticle force for small displacement, but does not retain terms that would result in dispersion. This yields $\partial v_1/\partial x + \nu_d\, v_1/C_L = -iA\omega_1[v_2 v_{\rm diff} + v_{\rm sum} v_2^*]/2C_L^2$, describing the spatial evolution of the amplitude v_1 of the first pump wave, measured as the particle speed. Here, ν_d is the gas friction; v_2, $v_{\rm sum}$, and $v_{\rm diff}$ are the amplitudes at ω_2, $\omega_1 + \omega_2$, and $\omega_2 - \omega_1$, respectively, and $A = (\kappa^3 + 3\kappa^2 + 6\kappa + 6)/(\kappa^2 + 2\kappa + 2)$ is a measure of the wave's nonlinearity for a Yukawa potential. The model also yields four similar equations for the amplitudes of the waves at: $2\omega_1$, ω_2, $\omega_1 + \omega_2$, and $\omega_2 - \omega_1$.

The main predictions of our theory of nonlinear wave mixing are as follows. First, waves propagating along a common axis can mix only if they travel in the same direction. Second, due to friction damping, the generation of combination frequencies requires that the pump amplitude must exceed a certain threshold, which we estimate as roughly $v_1(0) >$

$2\nu_d C_L A^{-1}[\omega_2(\omega_2 \pm \omega_1)]^{-1/2}$. Third, amplitudes at the combination frequencies increase with the pump amplitude and frequency (if $\omega = \pm C_L k$ is still satisfied).

We performed experiments to observe nonlinear mixing and its dependence on the pump wave's direction, amplitude, and frequency. Our apparatus, Fig. 1, uses a capacitively-coupled rf discharge plasma. To achieve a low damping rate, we used Ar at a pressure of 5 mTorr, so that the gas drag, which is accurately modeled [17] by the Epstein expression, was only $\nu_d = 0.87\ \mathrm{s}^{-1}$. The plasma was sustained by a 13.56 MHz rf voltage with a peak-to-peak amplitude of 168 V and a self-bias of -115 V.

The lattice consisted of a monolayer of microspheres suspended in the discharge. The particles had a diameter of $8.09 \pm 0.18\ \mu$m measured using TEM and a mass density 1.514 g/cm^3. We used the pulse technique of Ref. [18] to measure $C_L = 21.6 \pm 1.5$ mm/s, $Q = -9400 \pm 900\ e$, and $\lambda_D = 0.73 \pm 0.10$ mm at the particles' height. The triangular lattice had a diameter of about 60 mm, an interparticle spacing of $675 \pm 14\ \mu$m, and a pair correlation function $g(r)$ with many peaks and a translational order length of $16a$, indicating that the lattice was in an ordered state.

The particles were imaged through the top window by a video camera, and they were illuminated by a horizontal He-Ne laser sheet. We recorded movies of $68.3 - 136.7$ s duration on a digital VCR at 29.97 frames per second. The 24×18 mm field of view included $1000 - 1100$ particles, Fig. 1(a). The images were digitized with an 8-bit gray scale and a 640×480 pixel resolution. Particle coordinates and velocities were then calculated in each frame with sub-pixel spatial resolution using the moment method [19].

We used a laser-manipulation method [20] to excite two sinusoidal compressional pump waves with parallel wave fronts in the plasma crystal, as shown in Fig. 1. Particles were pushed by the radiation pressure force, which is proportional to an incident laser intensity [21]. An Ar^+ laser beam was split in two, and the intensity of each beam was sinusoidally modulated with a separate scanning mirror that partially blocked the laser beam. In this modulation method, second and third harmonics were present in the laser intensity with

$< 1\%$ compared to the fundamental frequency. The total power of the two laser beams incident on the lattice was varied up to 3.69 W. At their foci at the particle location, the laser beams had a diameter of 0.5 mm measured at the level of $1/e^2$ of their maximum intensity, at a power of 0.61 W. Two more scanning mirrors, oscillated rapidly at 200 Hz, were used to raster each of the two laser beams into sheets, which struck the lattice at an angle of 10° with respect to the horizontal lattice. The sheets extended 4.5 mm beyond each edge of the camera's field of view, and their intensity was uniform $\pm 10\%$ in the y direction within the field of view.

The excitation regions for the two pump waves were the stripes where the two laser sheets struck the lattice. The two stripes were separated by 5.5 mm in the x direction. Waves with parallel wavefronts propagated outward from each excitation region. The two stripes were parallel, so that the two pump waves propagated along a common axis, in opposite directions in the region between the stripes, and in the same direction elsewhere. We verified, by using a side-view video camera, that there was no out-of-plane buckling of our 2D lattice, thereby confirming that all the waves we observed were in-plane.

To analyze the wave propagation, we spatially averaged the x-component of the particle velocity within 40 rectangular bins elongated along the y axis. We then computed the power spectrum $|v_x(f)|^2$ for particle motion, for each of the 40 bins in the x direction.

One of our chief experimental results is an observation of sum and difference frequencies, Fig. 2(a). These combination frequencies are a signature of nonlinear mixing between the pump waves. Higher frequencies $2f_2 - f_1$, $2f_1 + f_2$, $2f_2 + f_1$, etc. are also present, but these are not necessarily evidence of four-wave mixing, because the pump waves' harmonics were present already in the excitation regions [15]. The baseline at 10^{-6} mm^2/s^{2}Hz indicates the broadband spectrum corresponding to random particle motion. We found that this level is an order of magnitude higher than without laser excitation, suggesting that some of the pump energy is ultimately deposited into random particle motion. The lattice's translational order was also degraded at the highest laser powers, to a value of $4a$.

We performed a 2D MD simulation using parameters similar to those of the experiment.

The particle's equation of motion was integrated for 5000 particles. The electric potential consisted of a harmonic potential for the external radial confinement plus a binary interparticle Yukawa repulsion. The laser force was chosen 9% smaller than calculated in Ref. [17], to match the amplitudes of the pump waves in the experiment.

Simulation results for the power spectrum $|v_x(f)|^2$ in Fig. 2(b) are similar to the experimental results in Fig. 2(a), suggesting that our simulation incorporated the essential physics of our experiment. However, the amplitudes of the peaks in Figs. 2(a),(b) do not all agree. While the amplitudes at f_1, f_2, $2f_1$, $2f_2$, $3f_1$, and $3f_2$ are similar, the amplitudes at the combination frequencies are smaller in the experiment than in the simulation. We cannot account exactly for this difference, but one possibility is that the actual interparticle potential is not exactly Yukawa.

The spatial profile of the sum-frequency wave in Fig. 3 reveals how energy is transferred from the pump waves to the wave at the sum frequency. Between the excitation regions, where the two pump waves propagate oppositely, the sum frequency is weak. Elsewhere, the two pump waves propagate in the same direction, and the sum-frequency amplitude grows with distance, as energy is extracted from the pump waves. In agreement with theory, the sum-frequency amplitude reaches a maximum value and then declines, due to pump depletion and damping. For the theoretical curves shown in Fig. 3(b), we solved the system of five equations to calculate $v_{\mathrm{sum}}(x)$, as well as $v_1(x)$, $v_2(x)$, $v_{\mathrm{diff}}(x)$, and $v_{2\omega_1}(x)$. We assumed both pump waves were excited at $x = 0$. We used experimental values for C_L, ν_d, A, $v_1(0)$, $v_2(0)$, $v_{\mathrm{sum}}(0)$, $v_{\mathrm{diff}}(0)$, and $v_{2\omega_1}(0)$, where the three latter values were assumed to be the thermal noise levels.

A threshold is seen in Fig. 4, as predicted by theory, so that the combination frequencies were present only when the excitation laser power P_{laser} was sufficient for nonlinear effect to overcome damping. While the amplitude at the pump is almost proportional to P_{laser}, the amplitude at the combination frequencies grew faster that linearly, above the threshold. For the sum-frequency in Fig. 4, the threshold value is ≈ 0.4 W, which agrees with the theoretical prediction in Fig. 3(b) of a threshold in the range of $0.23 - 0.61$ W.

Unlike the combination frequencies, the second harmonic $2f_1$ in Fig. 4 does not exhibit a threshold. We attribute this to the presence of the harmonics in the excitation regions [15]. While we did observe some indication of harmonic generation outside the excitation regions, we believe that the combination frequencies in Fig. 4 are a more convincing indication of three-wave mixing, because they were not present in the laser modulation.

Despite the dispersion relation not perfectly obeying $\omega \propto k$, so that one would expect wavenumbers not to match, we observed significant nonlinear mixing in the experiment. Apparently the phase-matching conditions for three-wave mixing are relaxed. We attribute this to damping and to finite size of the lattice and the excitation regions, which cause the wave's k-spectrum to have a finite width. We estimate that damping by itself allows mixing with a mismatch as large as $\Delta k = 2\nu_d/C_L$. Our theory, which includes none of these effects, predicts that the amplitudes at combination frequencies increase with frequency; we observed this trend in the experiment up to a maximum pump frequency of $\omega_2 = 1.1\omega_0$, beyond which dispersion becomes significant.

We thank F. Skiff and A. Bhattacharjee for valuable discussions and L. Boufendi for TEM measurements. This work was supported by NASA and DOE.

REFERENCES

[1] V.M. Kaganer, H. Mohwald, and P. Dutta, Rev. Mod. Phys. **71**, 779 (1999).

[2] C.C. Grimes and G. Adams, Phys. Rev. Lett. **42**, 795 (1979).

[3] P.A. Heiney *et al.*, Phys. Rev. Lett. **48**, 104 (1982).

[4] F.M. Peeters and X. Wu, Phys. Rev. A **35**, 3109 (1987).

[5] J.H. Chu and Lin I, Phys. Rev. Lett. **72**, 4009 (1994).

[6] H. Thomas *et al.*, Phys. Rev. Lett. **73**, 652 (1994).

[7] Y. Hayashi and K. Tachibana, Jpn. J. Appl. Phys. **33**, L804 (1994).

[8] A. Melzer, T. Trottenberg, and A. Piel, Phys. Lett. A **191**, 301 (1994).

[9] X. Wang, A. Bhattacharjee, and S. Hu, Phys. Rev. Lett. **86**, 2569 (2001).

[10] D.H.E. Dubin, Phys. Plasmas **7**, 3895 (2000).

[11] N.N. Rao, P.K. Shukla, and M.Y. Yu, Planet. Space Sci. **38**, 543 (1990).

[12] D. Samsonov *et al.*, Phys. Rev. Lett. **88**, 095004 (2002).

[13] K. Avinash *et al.*, submitted to Phys. Rev. E.

[14] V. Nosenko, S. Nunomura, and J. Goree, Phys. Rev. Lett. **88**, 215002 (2002).

[15] S. Nunomura *et al.*, submitted to Phys. Rev. E.

[16] U. Konopka, G.E. Morfill, and L. Ratke, Phys. Rev. Lett. **84**, 891 (2000).

[17] B. Liu *et al.*, Phys. Plasmas **10**, 9 (2003).

[18] V. Nosenko *et al.*, Phys. Rev. Lett. **88**, 135001 (2002).

[19] A. Melzer *et al.*, Phys. Rev. E **62**, 4162 (2000).

[20] A. Homann *et al.*, Phys. Rev. E **56**, 7138 (1997).

[21] A. Ashkin, Phys. Rev. Lett. **24**, 156 (1970).

FIGURES

FIG. 1. Experimental apparatus. (a) Particles arranged in a triangular 2D lattice. Atop this image is a sketch showing where the radiation pressure force from two modulated Ar^+ laser sheets pushes particles, exciting sinusoidal compressional pump waves. (b) The particles are polymer microspheres, levitated as a monolayer above the lower electrode in a capacitively-coupled rf plasma.

FIG. 2. Power spectrum of the particle speed $|v_x(f)|^2$ averaged over the camera's field of view, for the highest excitation laser power of 3.69 W, (a) experiment and (b) 2D MD simulation using Yukawa interparticle potential. Sinusoidal compressional pump waves were excited in the plasma crystal with frequencies $f_1 = 0.7$ Hz and $f_2 = 1.7$ Hz. In both experiment and simulation, combination frequencies and harmonics were generated at high excitation laser power, due to nonlinear mixing of the pump waves.

FIG. 3. Spatial profiles of the amplitude at the sum frequency, (a) experiment and (b) theory. Sinusoidal compressional pump waves with frequencies $f_1 = 0.7$ Hz and $f_2 = 1.7$ Hz were excited in the plasma crystal at the locations shown by arrows, which were spatially separated in the experiment but not the theory. In agreement with theory, amplitudes at combination frequencies grew where the pump waves propagated in the same direction.

FIG. 4. Wave amplitudes, averaged over the camera's field of view, as a function of the excitation laser power $P_{\rm laser}$. The amplitude of the pump waves at $f_1 = 0.7$ Hz and $f_2 = 1.7$ Hz was almost proportional to $P_{\rm laser}$. In agreement with theory, sum frequencies were generated only above an excitation-power threshold depending on the sum frequency. Pump wave harmonics were present at any $P_{\rm laser}$, due to imperfect modulation of the laser's intensity.

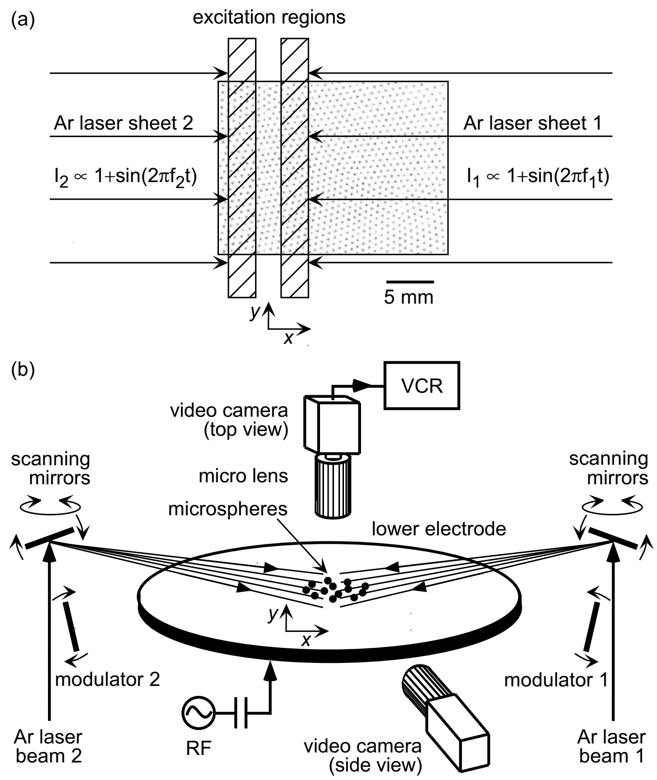

(a)
excitation regions
Ar laser sheet 2
$I_2 \propto 1+\sin(2\pi f_2 t)$
Ar laser sheet 1
$I_1 \propto 1+\sin(2\pi f_1 t)$
5 mm
y
x
(b)
VCR
video camera
(top view)
micro lens
microspheres
lower electrode
scanning
mirrors
scanning
mirrors
y
x
modulator 2
modulator 1
RF
video camera
(side view)
Ar laser
beam 2
Ar laser
beam 1

Fig. 1

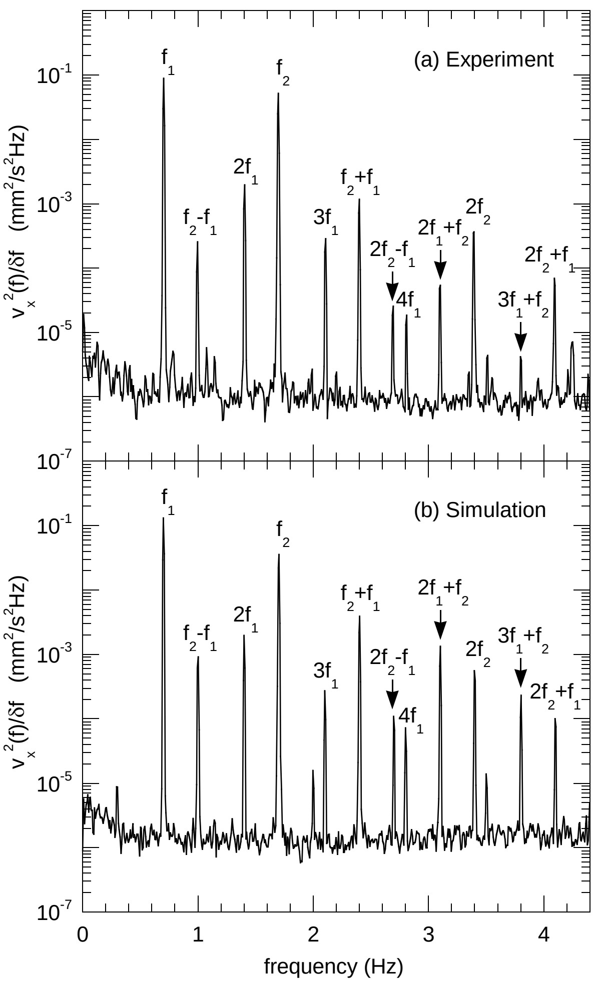
(a) Experiment
(b) Simulation
$v_x^2(f)/\delta f$ (mm^2/s^{2}Hz)
frequency (Hz)
f_1
f_2
f_2-f_1
$2f_1$
$3f_1$
f_2+f_1
$2f_2$-f_1
$4f_1$
$2f_1$+f_2
$2f_2$
$3f_1$+f_2
$2f_2$+f_1
10^{-1}
10^{-3}
10^{-5}
10^{-7}
0
1
2
3
4

Fig. 2

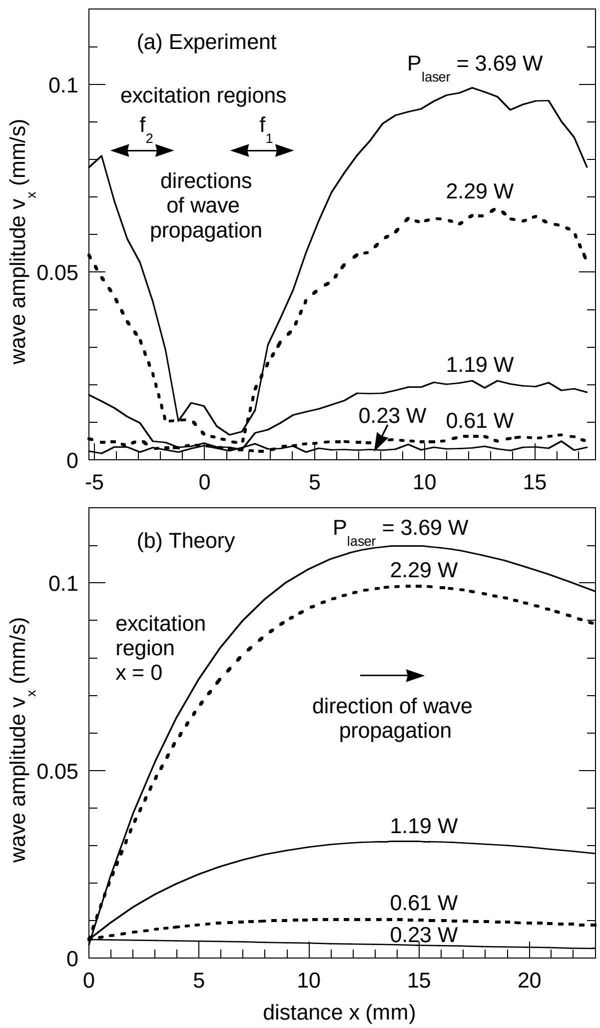
(a) Experiment
excitation regions
f2
f1
directions
of wave
propagation
Plaser = 3.69 W
2.29 W
1.19 W
0.23 W
0.61 W
wave amplitude vx (mm/s)
0
0.05
0.1
-5
0
5
10
15
(b) Theory
Plaser = 3.69 W
2.29 W
excitation
region
x = 0
direction of wave
propagation
1.19 W
0.61 W
0.23 W
wave amplitude vx (mm/s)
0
0.05
0.1
0
5
10
15
20
distance x (mm)

Fig. 3

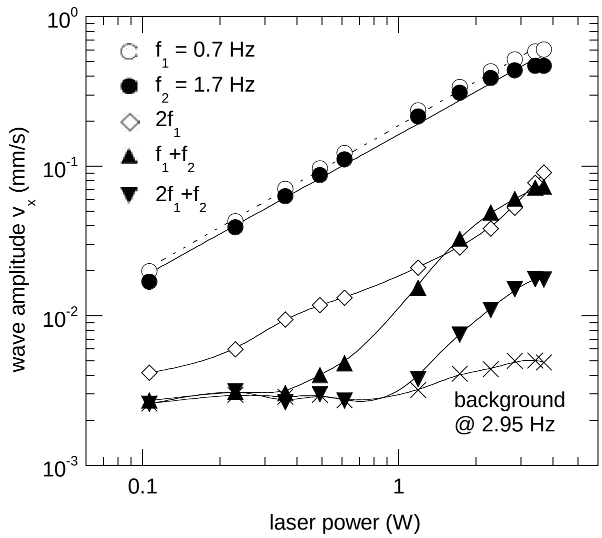
f1 = 0.7 Hz
f2 = 1.7 Hz
2f1
f1+f2
2f1+f2
background
@ 2.95 Hz
wave amplitude vx (mm/s)
laser power (W)
10^0
10^-1
10^-2
10^-3
0.1
1

Fig. 4